



Cite this: *Environ. Sci.: Water Res. Technol.*, 2022, **8**, 1287

Performance of biochars for the elimination of trace organic contaminants and metals from urban stormwater†

Stephanie Spahr, *^{abc} Marc Teixidó, ^{bde} Sarah S. Gall, ^{abf} James C. Pritchard, ^{ab}
Nikolas Hagemann, ^{gh} Brigitte Helmreich ^f and Richard G. Luthy *^{ab}

Urban stormwater carries dissolved organic and metal contaminants that pose risks to water supplies and the environment. Green infrastructure elements such as biofilters have the potential to capture and treat urban stormwater prior to infiltration to groundwater. Because conventional sand-based biofilters often fail to eliminate dissolved contaminants from stormwater, there is a need to improve biofilter treatment efficiency. In our study, we investigated four different wood-derived biochars for the removal of seven trace organic contaminants (TrOCs, atenolol, benzotriazole, dicamba, diuron, fipronil, mecoprop, terbutryn) and five metals (cadmium, copper, lead, nickel, zinc). Three biochars were produced at pyrolysis temperatures of 400 °C, 580 °C, and 750 °C, and one biochar of biomass gasification (1100–1400 °C). Batch experiments conducted with synthetic stormwater showed that the removal capacity of the biochars increased with increasing production temperature and specific surface area. The gasification biochar outperformed the three pyrolysis biochars and was further tested in flow-through column experiments operated for more than eight months and 4000 pore volumes. The least retained organic contaminant was dicamba followed by fipronil and terbutryn. Using a 1-D forward prediction intraparticle diffusion-limited sorption model, 20% breakthrough of dicamba was estimated to occur at 1100 and 5300 pore volumes in biochar-amended sand filters containing 1 to 10 weight percent biochar, respectively. Based on these results, case study calculations for a full-scale biochar filter in Los Angeles, CA, suggest potential service lifetimes of five years and longer when using dicamba as an indicator compound for early TrOC breakthrough.

Received 21st November 2021,
Accepted 11th April 2022

DOI: 10.1039/d1ew00857a

rsc.li/es-water

Water impact

Urban stormwater contains dissolved trace organic contaminants and metals that need to be removed to protect water supplies and aquatic ecosystems. This study combines laboratory batch and column experiments with transport modeling to assess the efficacy and longevity of biochar filters for urban stormwater treatment and highlights the need for improved biochar testing and selection strategies.

1. Introduction

Numerous cities across the world experience increasing water stress due to climate change, urbanization, and continuous introduction of anthropogenic contaminants in the urban

water cycle.¹ Stormwater runoff is a major contributor to surface water quality impairments as it can carry pollutants such as trash, pathogens, nutrients, metals, and trace organic contaminants (TrOCs).^{2–7} Large quantities of synthetic chemicals are used in the urban environment including

^a Department of Civil and Environmental Engineering, Stanford University, Stanford, California, USA. E-mail: luthy@stanford.edu

^b NSF Engineering Research Center for Re-inventing the Nation's Urban Water Infrastructure (ReNUWIt), USA

^c Department of Ecohydrology and Biogeochemistry, Leibniz Institute of Freshwater Ecology and Inland Fisheries (IGB), Berlin, Germany.
E-mail: stephanie.spahr@igb-berlin.de

^d Department of Civil and Environmental Engineering, University of California, Berkeley, California, USA

^e Institute of Environmental Assessment and Water Research, IDAEA-CSIC, Barcelona, Catalonia, Spain

^f Chair of Urban Water Systems Engineering, School of Engineering and Design, Technical University of Munich, Garching, Germany

^g Ithaka Institute, Freiburg, Germany

^h Agroscope, Zürich, Switzerland

† Electronic supplementary information (ESI) available: Chemicals, analytical parameters, synthetic stormwater composition, biochar characterization, statistical analyses, batch sorption experiments, column experiments (bromide tracer tests, water quality parameters, breakthrough curves for nickel, 1H-benzotriazole, and mecoprop), model equations and input parameters for the forward-prediction transport model, sorption parameters obtained from column breakthrough curve fitting, and case study to predict filter longevity. See DOI: <https://doi.org/10.1039/d1ew00857a>



pesticides, biocides in paints, and corrosion inhibitors in brake fluids and antifreeze.⁸ Many of these chemicals are water soluble compounds that may be mobilized during rain events and enter the aquatic environment *via* stormwater runoff. A number of these contaminants are persistent and mobile in water and can be transported further downstream or enter aquifers.⁹ Eventually, these chemicals may end up in drinking water either in their original form or as potentially harmful transformation products.

To protect aquatic ecosystems and human health from adverse effects caused by synthetic chemicals,^{10,11} new strategies are needed to prevent the entry of urban-runoff contaminants into surface waters and groundwater. While wastewater treatment plants can now be equipped with advanced treatment technologies using activated carbon or ozone to eliminate a large proportion of recalcitrant organic chemicals from wastewater effluent, stormwater will continue to challenge the urban water system.^{12–15}

Urban green infrastructure elements, also called best management practices, are being installed in cities to move toward a more sustainable and resilient urban water management regime.¹⁶ Urban green infrastructure including constructed wetlands or biofilters provide multiple benefits such as water retention for flood control, greening and cooling the city, habitat improvement for wildlife, and land appreciation.¹⁶ Green infrastructure elements also provide the potential for removal of contaminants from urban stormwater runoff.^{8,17} Biofilters, also known as infiltration swales, rain gardens, or bioretention cells, have received special attention as nature-based solutions for improved stormwater purification.^{18–21} While conventional sand-based biofilters can remove particle-associated pollutants, polar and mobile organic contaminants are often not reliably eliminated.^{8,22,23}

Biochar has gained increasing attention as a low-cost and sustainable adsorbent for the purification of stormwater.^{8,24–26} Biochar is a carbonaceous material that can be produced from biomass such as wood, agricultural waste, grass, or sludge by pyrolysis or gasification.^{27,28} Similar to activated carbon, biochar can adsorb organic contaminants and has also been shown effective for the removal of pathogens and metals from water.^{24,25,29–31} Commercial activated carbon used for water treatment is often produced from fossil carbon – peat, coal, or lignite – and requires energy intensive treatment with steam at high process temperatures above 900 °C. Biochar can be locally produced from residual biomass, is less costly, qualifies as a negative emission technology, and may co-generate energy (industrial heat, electricity) especially when produced by gasification.^{27,32,33} The physicochemical properties of biochar are highly variable as they depend on both feedstock selection and production conditions.²⁷ In a screening of commercially available biochars, Ulrich *et al.* 2015 found that a high-temperature gasification biochar performed best for the removal of organic contaminants from stormwater.³⁴ In contrast, biochars produced at low temperatures were

suggested to be more effective for the removal of inorganic contaminants.^{35,36} Currently, it remains challenging to select suitable biochars for the treatment of stormwater, which contains mixtures of organic and metal contaminants. Also, we lack standardized testing protocols to assess the performance of biochars as well as the longevity of biochar filters for stormwater purification.

The overarching goal of this study is to contribute towards (i) an improved biochar selection process for the removal of metals and TrOCs from urban stormwater and (ii) the identification of trace organic compounds that can serve as indicators for the performance and longevity of biochar filters. To this end, we systematically investigated the sorption of five metals and seven trace organic contaminants, which are relevant in stormwater runoff, onto four biochars produced at different treatment temperatures and processes. Experiments were carried out in synthetic stormwater containing dissolved organic carbon (DOC) in order to mimic realistic conditions. Moreover, we determined whether the co-presence of organic contaminants and metals affects their overall removal. After screening tests, flow-through column experiments were conducted with one weight percent (wt%) of the best-performing biochar mixed with either silica or limestone sand. The columns were fed for more than eight months with a mixture of the selected metals, DOC, and TrOCs to identify suitable indicator compounds for biochar performance. Lastly, we present results from transport modeling of breakthrough curves using a 1-D intraparticle diffusion-based sorption model, and predict the potential lifetime of full-scale stormwater filters containing 1 wt%, 2.5 wt%, 5 wt%, and 10 wt% of biochar using the least retained organic contaminant as a conservative indicator for filter longevity.

2. Materials and methods

A list of all chemicals including suppliers and purities is provided in the ESI† (Table S1).

2.1 Biochar and sand

Three biochars were produced from a mix of spruce and fir wood at constant pyrolysis temperatures of 400 °C (BC400), 580 °C (BC580) and 750 °C (BC750) in a continuous pyrolysis process with a residence time of 10 min on a PYREKA pyrolysis unit.³¹ One conifer softwood biochar was obtained from a commercial gasification plant operating at temperatures up to 1100–1400 °C (Mountain Crest Gardens, MCG, GrowPro Inc., California, USA). All biochars were analyzed for their specific surface area (SSA) and their elemental composition by Eurofins Umwelt Ost GmbH, Germany, according to the guidelines of the European Biochar Certificate.²⁸ The MCG biochar was further analyzed with Hg porosimetry to determine the pore size distribution (TU Freiberg, Germany). Ottawa (silica) sand (Fisher Scientific) was washed with 5% HNO₃ for 24 hours and rinsed several times with DI water until neutral pH.



Commercial limestone sand (VICAL, Minerals Technologies, USA) consisting of CaCO_3 (97%) with traces of MgCO_3 (1.2%) and Fe_2O_3 (0.05%) was used as received. Sand and biochar were sieved to 0.595–0.841 mm (*i.e.*, 20–30 Tyler mesh size).

2.2 Synthetic stormwater

Batch and column experiments were performed with synthetic stormwater emulating the composition of actual stormwater.³⁷ The simulated stormwater matrix contained 4.4 mg L^{-1} NO_3^- , 1.3 mg L^{-1} NH_4^+ , 1.5 mg L^{-1} H_2PO_4^- , 31 mg L^{-1} SO_4^{2-} , 60 mg L^{-1} HCO_3^- , 1.8 mg L^{-1} Mg^{2+} , 30 mg L^{-1} Ca^{2+} , 40 mg L^{-1} Na^+ , and 61 mg L^{-1} Cl^- (Table S4†).³⁷ The dissolved organic carbon (DOC) concentration was set at 5 mg C L^{-1} . Suwannee river natural organic matter (International Humic Substances Society, St. Paul, MN) was used for all batch experiments. As Suwannee river natural organic matter could not be provided in sufficient quantity for the long-term column experiments, we used humic acid (Sigma Aldrich) as an organic carbon source for the flow-through studies where the actual applied concentration ranged from 2 to 4 mg C L^{-1} DOC. The pH of the synthetic stormwater was adjusted to 7.5.

2.3 Batch sorption experiments

2.3.1 Biochar screening for sorption of metals. Sorption of five dissolved metals (Cd, Cu, Ni, Pb, and Zn, all co-present in the solution) on the four biochars was investigated using batch reactors containing 5 mg, 20 mg, or 40 mg of biochar in 200 mL of synthetic stormwater, and 15 mg, 20 mg, or 25 mg of biochar in 50 mL of synthetic stormwater corresponding to 0.025, 0.1, 0.2, 0.3, 0.4, and 0.5 g biochar per L, respectively. Batch reactors were placed on a shaker table in the dark for 48 hours to wet the biochar prior to the addition of metals. One metal stock solution containing all five metals in dissolved form at 50 mg L^{-1} was prepared from weighting in CdCl_2 , CuCl_2 , NiCl_2 , PbCl_2 , and ZnCl_2 in DI water acidified with 1 volume percent of HNO_3 . Each biochar batch reactor was spiked with the stock solution to achieve an initial concentration for each metal of 50 $\mu\text{g L}^{-1}$. A control experiment was set up without biochar to assess negligible losses of metals in the synthetic stormwater matrix. The pH was monitored over time and remained stable at 7.5. After 48 hours, 10 mL of sample was filtered with a 0.45 μm PES syringe filter (TISCH Scientific), spiked with 300 μL of 65–70% HNO_3 , and stored in the dark at 4 °C until analysis.

2.3.2 Biochar screening for sorption of TrOCs. The sorption of seven TrOCs (1H-benzotriazole, atenolol, dicamba, diuron, fipronil, mecoprop, and terbutryn, all co-present in the solution) was evaluated with the four biochars in batch reactors containing 5 mg, 20 mg, or 40 mg of biochar in 200 mL of synthetic stormwater at pH 7.5 corresponding to a solid-to-liquid ratio of 0.025, 0.1, and 0.2 g biochar per L, respectively. The organic contaminants were chosen based on reported occurrence in urban stormwater,⁸ usage types (including a corrosion inhibitor, herbicides, biocides, an

insecticide and a pharmaceutical, which may serve as indicator for stormwater impacted by human sanitary sewage), and physicochemical properties (including anionic, neutral, and cationic species, Table S2†). The log octanol–water partition coefficients ($\log K_{\text{OW}}$ for neutral compounds) and log octanol–water distribution coefficients ($\log D_{\text{OW}}$ values for ionizable compounds) were below 4 indicating their aquatic mobility. Batch reactors were placed on a shaker table at 200 rpm for 48 hours to wet the biochar prior to the addition of organic contaminants. Subsequently, 100 μL of a 0.2 g L^{-1} methanolic TrOC solution containing all seven TrOCs was spiked to achieve an initial concentration of 100 $\mu\text{g L}^{-1}$ of each compound. A control experiment was set up without biochar to assess negligible losses of TrOCs in the synthetic stormwater matrix. After 48 hours, 1.5 mL of sample was filtered with a 0.45 μm GF syringe filter (TISCH Scientific) and stored in the dark at 4 °C until analysis.

2.3.3 Sorption of TrOCs and metals on BC750 and MCG biochar. The two best-performing biochars (BC750 and MCG) were further applied to study sorption of (i) the mixture of seven TrOCs only, (ii) the mixture of five metals only, and (iii) all seven TrOCs and five metals in co-presence over a time span of seven days in synthetic stormwater at pH 7.5. Sorption of TrOCs ($c_0 = 50 \mu\text{g L}^{-1}$, each) and metals ($c_0 = 50 \mu\text{g L}^{-1}$, each) was determined in batches with 0.025 g biochar per L and 0.2 g biochar per L, respectively. Experiments in co-presence of seven TrOCs and five metals ($c_0 = 50 \mu\text{g L}^{-1}$, each) were performed using both 0.025 and 0.2 g biochar per L. Control batches without biochar were set up to investigate interactions between metals and TrOCs ($c_0 = 50 \mu\text{g L}^{-1}$, each) in aqueous solution. All sorption experiments were conducted in triplicates with daily measurements to confirm sorption plateau at seven days (ESI† section S6).

2.4 Flow-through column experiments

Twelve columns of 48 cm length and 3.175 cm inner diameter (clear PVC pipes with PVC pipe connectors) were operated to test four different geomedia configurations in triplicates: (i) silica (Ottawa) sand, (ii) silica sand mixed with 20 wt% carbonate sand (limestone), (iii) silica sand mixed with target 1 wt% (exact 0.87 wt%, corresponding to 8.4 volume percent) MCG biochar, and (iv) silica sand mixed with 20 wt% carbonate sand and target 1 wt% MCG biochar (Fig. 1). Three-way diverting sampling valves were installed at the outlet of the columns. The columns were operated in up-flow mode at a flow rate of 1.2 mL min^{-1} (Darcy velocity of 9 cm h^{-1}) using a multi-channel peristaltic pump (Sci-Q 205 U, Watson-Marlow) and semi-clear PTFE tubing (0.3175 cm inner diameter). The flow rate emulated the recharge conditions at a stormwater wetlands park in Los Angeles, CA, USA³⁸ at which $1.1 \times 10^6 \text{ m}^3$ stormwater will be captured over 4 months during the rainy season. The stormwater will be stored in constructed ponds and wetlands, which act as a hydraulic buffer for flow control.³⁸ Our column studies simulate filters operated with constant water flow after the



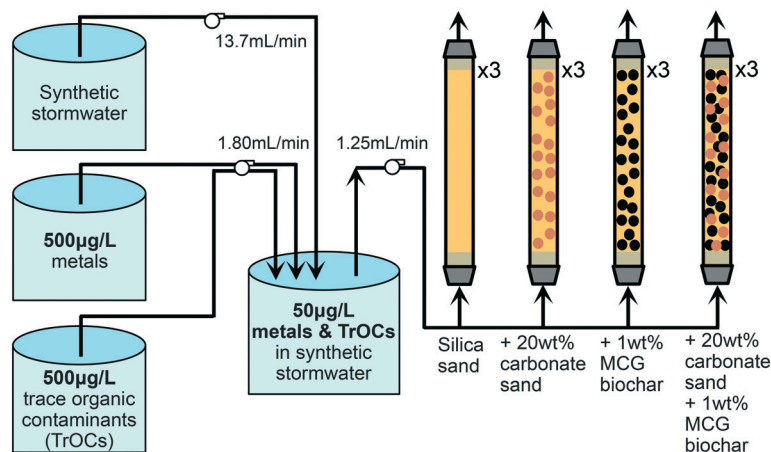


Fig. 1 Experimental setup of the column flow-through experiments with synthetic stormwater at pH 7.5 containing metals (Cd, Cu, Ni, Pb, Zn, each $50 \mu\text{g L}^{-1}$) and TrOCs (1*H*-benzotriazole, atenolol, dicamba, diuron, fipronil, mecoprop, terbutryn, each $50 \mu\text{g L}^{-1}$). The synthetic stormwater contained inorganic constituents and 5 mg C L^{-1} DOC.

wetlands. We assume a filter size of 4047 m^2 to treat the captured stormwater prior to infiltration for groundwater recharge. While we envision the biochar filters to run under saturated conditions during the rainy season with flow control, the filters are expected to dry out during the summer months. However, it was beyond the scope of this study to assess dynamic wet/dry seasonal operation of the filters.

Detailed information on the porosity of the filter material and pore volume determination as well as bromide tracer tests can be found in the ESI† (section S7). After an initial equilibration time of five days with synthetic stormwater, TrOCs and metals were introduced into the columns for 263 days according to the experimental setup depicted in Fig. 1. Synthetic stormwater (pH 7.5) spiked to achieve 5 mg C L^{-1} DOC was prepared weekly in a 200 L tank and pumped with a flow rate of 13.7 mL min^{-1} into a mixing chamber. Once per week, we freshly prepared two stirred 20 L tanks containing a $500 \mu\text{g L}^{-1}$ TrOC mixture and a $500 \mu\text{g L}^{-1}$ metal mixture in DI water, respectively. One multi-channel peristaltic pump independently transported the two contaminant solutions to a mixing chamber (a 20 L glass tank) resulting in a final concentration of $50 \mu\text{g L}^{-1}$ of each TrOC and metal being pumped into the columns. The mixing chamber was continuously air-bubbled and all pumps were remotely controlled using a single-board microcontroller (Arduino Uno SMD R3). To minimize stagnancy, the residence time in the mixing chamber was approximately 8 hours. At pre-selected time points, concentrations of metals and TrOCs were determined in influent samples (c_0 , collected from the mixing chamber, Fig. S16 and S19†) and effluent samples (c , collected at the column outlet) to calculate removal efficiencies (c/c_0). Breakthrough of metals and TrOCs was defined as c divided by c_0 equals 0.2. Selected samples were further analyzed for dissolved organic carbon (TOC-L Shimadzu, section S7.3†), dissolved oxygen (ProODO, YSI, section S7.4†), nutrients (SmartChem Discrete Analyzer, Westco Scientific Instruments, section S7.5†), pH, oxidation-

reduction potential, electrical conductivity, total dissolved solids, and temperature (multi-parameter probe, HANNA Instruments), and turbidity (HANNA Instruments, section S7.6†). All columns remained oxic throughout the experimental run time and no removal of dissolved organic carbon or nutrients was observed. A detailed description on water quality analyses can be found in the ESI† (section S7).

2.5 Chemical analyses

Metal analysis. Cd, Cu, Ni, Pb, and Zn were quantified using an inductively coupled plasma mass spectrometer (ICP-MS, Thermo Scientific XSERIES 2 Quadrupole). A sample volume of 10 mL was filtered with PES syringe filters (TISCH Scientific) and acidified with 300 μL of HNO_3 (65–70%) to obtain 2 vol% of HNO_3 in each sample prior to analysis. A 10 mg L^{-1} stock solution (Inorganic Ventures, VA, USA) containing 5% v/v HNO_3 was diluted to generate an external calibration curve from $1 \mu\text{g L}^{-1}$ to $75 \mu\text{g L}^{-1}$ for Cd, Cu, Ni, Pb, and Zn analysis. Subsets of twelve samples were bracketed with quality control standards of $50 \mu\text{g L}^{-1}$. Limits of quantification were between $1.4 \mu\text{g L}^{-1}$ and $1.8 \mu\text{g L}^{-1}$.

TrOC analysis. TrOCs were quantified using liquid chromatography electrospray ionization tandem mass spectrometry (LC-ESI-MS/MS, Applied Biosystems API 3000) with a Shimadzu SCL-10AVP system controller and a SIL-20A autosampler (Shimadzu). 1*H*-Benzotriazole, atenolol, diuron, and terbutryn were quantified in positive ionization mode; fipronil, dicamba, and mecoprop in negative mode (Table S3†). Aqueous samples were analyzed using a XBridge BEH C18 column ($5 \text{ cm} \times 2.1 \text{ mm}$, $3.5 \mu\text{m}$, Waters) equipped with a XBridge BEH C18 VanGuard cartridge ($5 \text{ mm} \times 2.1 \text{ mm}$, $3.5 \mu\text{m}$, Waters). The mobile phase consisted of HPLC-grade water (solvent A, Optima LC/MS grade, Fisher Chemical) and methanol (solvent B, Optima, > 99.9%, Fisher Chemical) each acidified with 0.1 vol% formic acid. The eluent gradient for negative ionization mode was 10% B (0–4 min), linear



increase to 95% B at 12 min, and 95% B for 1 min at a flow rate of 200 $\mu\text{L min}^{-1}$. The eluent gradient for positive ionization mode was 10% B (0–0.02 min), linear increase to 67% B at 12 min, linear increase to 95% B at 13 min and 95% B for 1 min at a flow rate of 200 $\mu\text{L min}^{-1}$. Quantification of analytes was carried out using deuterated internal standards (final concentration of 10 $\mu\text{g L}^{-1}$, Table S3†) and external calibration standards ranging from 1 $\mu\text{g L}^{-1}$ to 100 $\mu\text{g L}^{-1}$. The limit of quantification was defined as the lowest concentration standard with a signal to noise ratio ≥ 10 . Data analyses were performed with the Analyst 1.5.2 software (AB Sciex).

2.6 Modeling of TrOCs in biochar filters and case study to predict filter longevity

To simulate and predict breakthrough times of TrOCs in biochar filters, a 1-D forward-prediction transport model was adapted from Werner *et al.* 2006 and 2012,^{39,40} and Ulrich *et al.* 2015.³⁴ The model is based on the Freundlich equation and describes sorption-retarded intraparticle diffusion kinetics as outlined in previous studies.^{34,39,40} Model equations and input parameters used to predict contaminant breakthrough in biochar filters are compiled in the ESI† (section S10, Table S28). Breakthrough data for the columns containing sand mixed with 1 wt% (exact 0.87 wt%) MCG biochar were fitted to the 1-D intraparticle diffusion limited sorption model to obtain the Freundlich coefficient (K_{fr}), the Freundlich exponent ($N = 1/n_{fr}$), and the intraparticle tortuosity (τ) of the biochar particles. Standard deviations for the parameters were calculated through separate fitting of the three individual columns (Table S29†). The case study calculations were based on the recharge conditions at the above described stormwater wetland in Los Angeles³⁸ assuming a filter area of 4047 m^2 , a filter depth of 1 m, and an annual infiltration period of 122 days (Table S30†).

3. Results and discussion

3.1 Impact of biochar characteristics on metal and TrOC removal

Batch screening tests with four wood-derived biochars were conducted to study the effect of biomass conversion conditions and processes (*i.e.*, pyrolysis and gasification) on the adsorbent removal capacity. Fig. S1 and S2† show the results for the removal of metals and TrOCs, respectively, by the three pyrolysis biochars BC400, BC580, and BC750 and the MCG gasification biochar. The contaminant removal

efficiency increased with heat treatment temperature, with the MCG gasification biochar exhibiting the best performance. BC400 and BC580 showed little removal of metals and TrOCs (<30%) at the tested solid-to-water ratios. In contrast, BC750 and the MCG biochar exhibited higher removal capacities towards all tested metals and TrOCs, and the contaminant removal efficiency increased with increasing solid-to-water ratio.

The physicochemical characteristics of the four biochars are shown in Table 1. The specific surface areas (SSA) of BC400 and BC580 were less than 100 $\text{m}^2 \text{g}^{-1}$, while the SSAs of BC750 and MCG biochar were 400 and 610 $\text{m}^2 \text{g}^{-1}$, respectively. With increasing pyrolysis temperature, the carbon content and the ash content of the biochars increased nonlinearly, and the hydrogen and oxygen contents displayed a nonlinear decrease. Consequently, the H/C, O/C and (N + O)/C molar ratios decreased with increasing pyrolysis temperature. Of all chars, the gasification MCG biochar displayed the highest ash content, specific surface area, and total pore volume obtained by BET analysis (Table 1 and S5†), as well as the smallest H/C molar ratio indicating a high degree of carbonization.

To identify which physicochemical properties are most related to contaminant removal, we correlated $\log K_d$ values with the biochar properties (see Tables S7 and S8† for linear semi-log correlation coefficients). For all metals (except Pb) and TrOCs, the adsorption strength significantly increased with increasing specific surface area of the biochars ($p < 0.05$). Moreover, a high degree of carbonization (expressed as low H/C molar ratio) enhanced contaminant removal ($p < 0.05$ to $p < 0.2$). A positive correlation between ash content and contaminant $\log K_d$ values was apparent but less pronounced ($p < 0.2$). These observations agree with previous findings concluding that aromatic carbon within hydrophobic structures were the main contributors to contaminant adsorption.^{34,41–43}

In 48 hour batch experiments, metal uptake followed the order $\text{Pb} > \text{Cu} > \text{Zn} > \text{Ni} \sim \text{Cd}$ (Fig. S1†) reflecting the hydrolytic properties of the metals. Metal removal followed the same order as the first hydrolysis constants indicating that a lower degree of solvation facilitates the approach and interactions with the biochar surface functional groups (*e.g.*, carboxyl and hydroxyl groups).⁴⁴ This removal sequence of metals has been observed with other carbonaceous materials such as granulated activated carbon, and the adsorption extent was ascribed to weak intermolecular (van der Waals forces) and electrostatic interactions between metals and

Table 1 Specific surface area (SSA), ash content, and elemental composition of three pyrolysis biochars produced at 400 °C, 580 °C, and 750 °C, and one gasification biochar (MCG). All values are related to biochar dry mass

	SSA ($\text{m}^2 \text{g}^{-1}$)	Ash (%)	Hydrogen (%)	Carbon (%)	Nitrogen (%)	Oxygen (%)	Sulfur (%)	H/C ratio	O/C ratio	(N+O)/C ratio
BC400	94	1.0	2.2	79.8	0.13	16.8	0.05	0.329	0.158	0.159
BC580	29	1.5	1.7	88.7	0.21	7.8	0.04	0.228	0.066	0.068
BC750	400	1.8	0.5	91.3	0.21	6.2	0.04	0.065	0.051	0.053
MCG	610	9.2	<0.1	82.9	0.15	7.9	0.08	0.014	0.072	0.073



surface functional groups.^{45,46} Ash content may also enhance metal removal.⁴⁴

Batch sorption experiments with BC750 and MCG biochar showed that diuron was the best removed TrOC followed by 1H-benzotriazole, atenolol, terbutryn, and fipronil (Fig. S2†). Several studies highlighted the high uptake capacity of biochar and soil organic matter for the herbicide diuron.^{25,34}

In contrast, the anionic species dicamba and mecoprop were less well removed, which may be due to greater electrostatic repulsion with the biochar functional groups bearing negative charge at the studied pH value.⁴⁵ The $\log K_d$ values were neither correlated with the molecular hydrophobicity (commonly measured by the octanol–water partition coefficient, Table S2†), nor with the mobility in soil (*i.e.*, the K_{OC} , Table S2†). TrOC sorption onto biochar is governed by multiple retention mechanisms at the surface including π – π electron donor–acceptor interactions, H-bonding, electrostatic interactions, and physical interactions such as pore-filling mechanisms.⁴⁵

The selected biochars removed metals to a lesser extent than TrOCs (Fig. S1 and S2†). Our results confirm that high temperature biochars with high specific surface area, hydrophobicity, and microporosity perform well for the removal of dissolved organic contaminants from

stormwater.⁴⁶ However, our results contradict the hypothesis that low-temperature biochars are more suitable for the removal of charged contaminants such as metals. Therefore, mixing different pyrolysis temperature biochars with gasification biochar was not considered.

3.2 Sorption in co-presence of metals and TrOCs

As BC750 and MCG outperformed the lower-temperature biochars in terms of metal and TrOCs removal from synthetic stormwater, these two biochars were chosen for subsequent experiments to determine 7 day sorption uptake of (i) metals only, (ii) TrOCs only, and (iii) metals and TrOCs together. Control experiments with $50 \mu\text{g L}^{-1}$ metals and $50 \mu\text{g L}^{-1}$ TrOCs together without biochar showed no removal of any metal or organic compound within 7 days (Fig. 2). The contaminant decrease in biochar systems can, thus, be assigned to interactions of metals and TrOCs with the carbonaceous adsorbents.

In batches containing 0.2 g biochar per L and $50 \mu\text{g L}^{-1}$ metals, the removal order was $\text{Pb} \sim \text{Cu} > \text{Zn} > \text{Ni} \sim \text{Cd}$ (Fig. 2a). The presence of $50 \mu\text{g L}^{-1}$ TrOCs significantly decreased the removal efficiency for Zn, Ni, and Cd for both biochars ($p < 0.05$, Table S9†) by up to 35%, 10%, and 15%,



Fig. 2 Batch experiments in co-presence of five metals (nominal initial concentration $c_0 = 50 \mu\text{g L}^{-1}$, each) and seven TrOCs ($c_0 = 50 \mu\text{g L}^{-1}$, each) with (a) 0.2 g biochar per L to determine sorption of metals, and (b) 0.025 g biochar per L to determine sorption of TrOCs onto BC750 or MCG biochar after a contact time of 7 days in synthetic stormwater at pH 7.5 with 5 mg C L^{-1} DOC. Reported is the concentration c measured after 7 days relative to the initial concentration c_0 for metals and TrOCs measured in the respective control batches without biochar. Error bars represent standard deviations of triplicate experiments. Asterisks represent statistical differences between bracketed treatments ($p < 0.05$).



respectively. The removal of Pb and Cu was not significantly affected by the presence of TrOCs ($p > 0.2$, Fig. 2a). The removal order for the co-presence of metals and TrOCs was altered to $Pb > Cu > Ni \sim Cd > Zn$. As shown in Fig. S4,† all TrOCs except dicamba were strongly adsorbed onto both BC750 and the MCG biochar within 7 days and removed to concentration levels below our detection limit.

In batches containing 0.025 g biochar per L and $50 \mu\text{g L}^{-1}$ TrOCs, the presence of $50 \mu\text{g L}^{-1}$ metals led to observable trends of decreased TrOC removal on both BC750 and MCG biochar (Fig. 2b, Table S11†). However, the co-presence of TrOCs and metals increased the dispersion of the data, and no significant differences in TrOC removal efficiency could be determined when comparing TrOC sorption onto biochars in absence and presence of metals ($p > 0.05$, Table S10†), with the only exception of terbutryn and atenolol (Fig. 2b).

Experiments with metals and TrOCs in co-presence confirm that MCG biochar has the highest adsorption capacity for both TrOCs and metals. Flow-through column experiments were, therefore, conducted only with the MCG biochar. The results presented in Fig. 2 corroborate that the concentrations of metals and TrOCs (each $50 \mu\text{g L}^{-1}$) remain

stable in synthetic stormwater over a time period of at least 7 days. This allowed the column experiments to be conducted with weekly replenishment of the influent mixture of metals and TrOCs.

3.3 Metal removal in flow-through column experiments

Metals were poorly removed from stormwater in flow-through column systems which agrees with the batch sorption experiments. Nickel was the least retained metal in sand and biochar-amended columns (Fig. S15†) with breakthrough (defined as $c/c_0 = 0.2$) in less than 20 pore volumes for silica sand and carbonate sand columns. Nickel breakthrough in biochar columns occurred after 120–160 pore volumes. Similar to Ni, Cd was poorly removed in both sand and biochar systems (Fig. 3a). The addition of carbonate sand led to a slight enhancement of Cd removal (breakthrough after 130 pore volumes) compared to silica sand (breakthrough after 30 pore volumes). The amendment of 1 wt% MCG biochar to silica sand increased Cd retention by approximately 100 pore volumes. The combination of 1 wt%

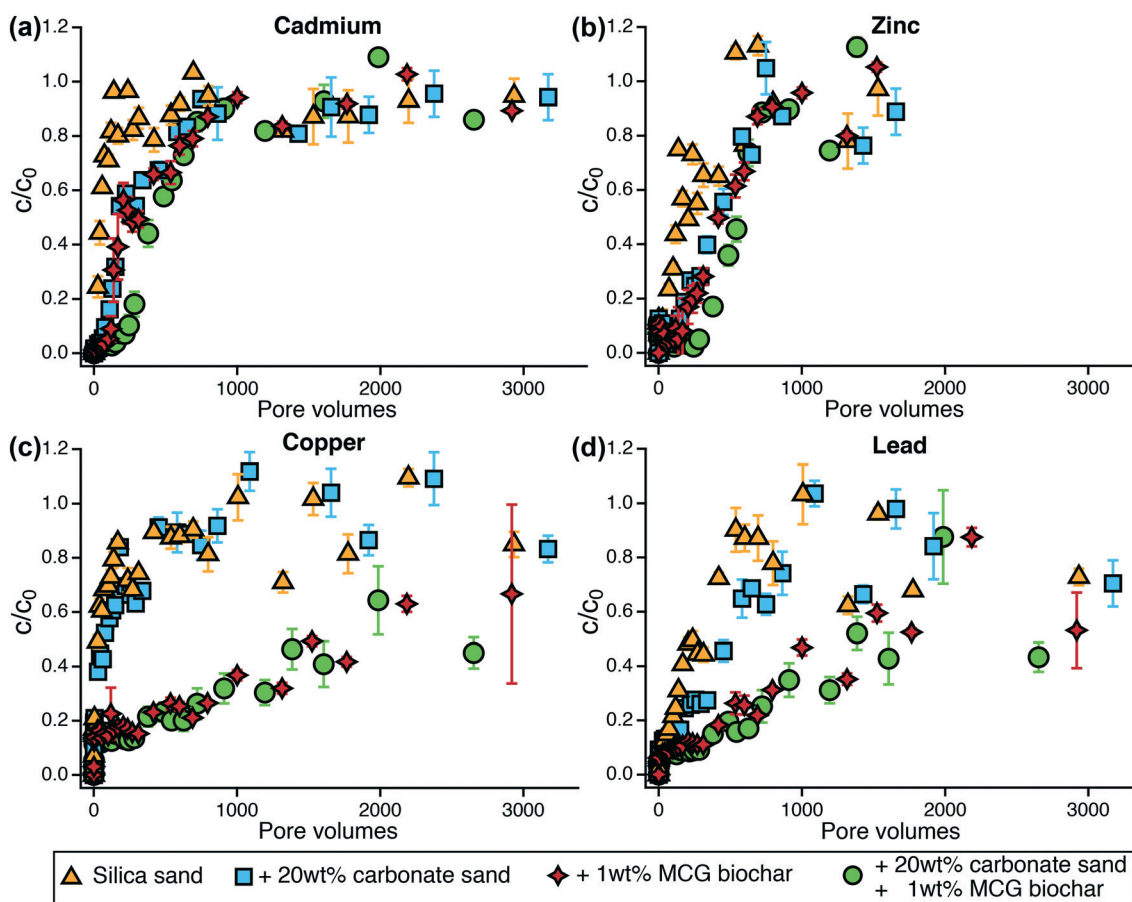


Fig. 3 Breakthrough of (a) cadmium, (b) zinc, (c) copper, (d) lead (initial nominal concentration $c_0 = 50 \mu\text{g L}^{-1}$) from synthetic stormwater (pH 7.5) in columns filled with (i) silica sand, (ii) silica sand mixed with 20 wt% carbonate sand, (iii) silica sand mixed with 1 wt% MCG biochar, and (iv) silica sand mixed with 20 wt% carbonate sand and 1 wt% MCG biochar. The concentrations c and c_0 were measured at the column effluents and in the mixing chamber, respectively. Error bars represent standard deviations of triplicate column systems.



MCG with 20 wt% carbonate sand showed best performance and removed 80% of the Cd for 280 pore volumes.

Zinc was slightly better removed than Ni and Cd (Fig. 3b). In silica and silica-carbonate columns, breakthrough of Zn was obtained after 70 and 170 pore volumes, respectively, indicating that carbonate sand also enhanced Zn retention ($p < 0.05$, Table S26†). The addition of 1 wt% MCG biochar to silica sand improved Zn removal by 190–240 pore volumes (breakthrough after 260 and 410 pore volumes in silica-biochar and silica-carbonate-biochar systems, respectively). Copper was not removed in silica or silica-carbonate sand systems as shown by immediate

breakthrough within 5 pore volumes (Fig. 3c). The formation of dissolved complexes with humic acid may have reduced Cu removal.⁴⁷ The amendment of 1 wt% MCG biochar to silica sand and silica-carbonate sand significantly improved Cu removal ($p < 0.05$, Table S26†) and breakthrough was observed after approximately 450 pore volumes (Fig. 3c). Lead was the best retained metal in both sand and biochar-amended systems (Fig. 3d). Silica sand and silica-carbonate sand removed 80% of lead for 100 and 170 pore volumes, respectively. Mixtures of silica sand and silica-carbonate sand with 1 wt% MCG resulted in 80% lead removal for 460 and 660 pore volumes, respectively.



Fig. 4 Breakthrough of (a) dicamba, (b) fipronil, (c) terbutryn, (d) diuron, and (e) atenolol (initial nominal concentration $c_0 = 50 \mu\text{g L}^{-1}$) from synthetic stormwater at pH 7.5 in columns containing (i) silica sand, (ii) silica sand mixed with 20 wt% carbonate sand, (iii) silica sand mixed with 1 wt% MCG biochar, and (iv) silica sand mixed with 20 wt% carbonate sand and 1 wt% MCG biochar. The concentrations c and c_0 were measured at the column effluents and in the mixing chamber, respectively. Error bars represent standard deviations of triplicate column systems.



In sum, for silica and carbonate sand-containing columns, copper, nickel, and cadmium showed immediate breakthrough followed by zinc and lead, which were slightly better retained. While carbonate sand has been reported to enhance the removal of metals,⁴⁸ the addition of 20 wt% carbonate sand to silica sand did not lead to improvements for metal removal in our study. Biochar increased the retention of metals compared to sand-only systems ($p < 0.05$, Table S26†) in the order of $Pb > Cu > Zn > Cd \geq Ni$. This order of sorption affinity matches findings in literature,^{48–50} and is consistent with our 48 hour batch sorption experiments where lead and copper were best removed by MCG biochar. In agreement with other studies,²⁵ biochar amendments to conventional sand filters are beneficial to enhance copper removal, which may be benefited by humic acid as shown previously.^{51,52} The biochar achieved about 50% removal of Cu and Pb through the duration of the tests in which metal concentrations were measured comprising about 3000 pore volumes.

3.4 TrOC removal in flow-through column experiments

TrOC removal was assessed in flow-through tests with measurements continuing for more than 4000 pore volumes. None of the TrOCs were retained by silica sand or carbonate sand so that the influent and effluent concentrations in the sand control columns were identical within the first few pore volumes (Fig. 4). Sand mixed with 1 wt% MCG biochar significantly enhanced the removal of organic contaminants ($p < 0.05$, Table S27†) even though bulk dissolved organic carbon was not removed (Table S13, Fig. S10†). In agreement with our batch sorption experiments, dicamba showed the earliest breakthrough, followed by fipronil and terbutryn. Diuron was the best retained TrOC and did not show breakthrough within the study time.

The type of sand (silica or carbonate) for mixing with the biochar did not lead to differences in the compound's retention behavior. The anionic species dicamba was the least retained compound in the organic contaminant mixture and showed breakthrough (defined as $c/c_0 = 0.2$) after 1300 pore volumes and complete breakthrough after approximately 3600 pore volumes (Fig. 4a). Fipronil and terbutryn were fully retained for 2000 pore volumes until a slow increase in concentration in the column effluent was observable. Twenty percent fipronil breakthrough was achieved after 2900 pore volumes (Fig. 4b). Subsequently, the breakthrough curve leveled off and no further increase in fipronil concentration could be measured in the column effluent. As the fipronil influent concentration remained stable between 40 and 60 $\mu\text{g L}^{-1}$ (Fig. S19†) and the column effluents were oxalic throughout the experiment (Table S15†), this observation may be assigned to aerobic (bio)transformation processes in the biochar columns. Towards the end of the column experiment, the fipronil concentration started to decline in both of the sand control systems (Fig. 4b) providing further evidence for potential (bio)transformation. However, the

identification of transformation products and underlying reaction mechanisms was beyond the scope of this study. Terbutryn concentrations in the column effluents increased steadily resulting in 12% breakthrough after 4000 pore volumes (Fig. 4c). Diuron and atenolol were continuously fed into the columns (Fig. S19†) and were completely removed by MCG biochar over the time course of the experiment (Fig. 4d and e).

The negatively charged mecoprop was expected to be poorly retained by biochar as shown in batch experiments but the compound dissipated within 300 pore volumes in the sand control columns indicating transformation processes (Fig. S17†). No breakthrough of mecoprop was observed in biochar columns, which may be attributed to sorption and potential transformation processes (Fig. S17†). Moreover, within the first 1000 pore volumes, the concentration of mecoprop gradually decreased in the mixing chamber (Fig. S19†) indicating degradation even prior to entering the columns. However, additional studies are needed to characterize the fate of mecoprop in such units. 1*H*-benzotriazole showed immediate breakthrough in the sand columns but after 800 pore volumes the compound disappeared in all sand systems (Fig. S18†) despite constant input into the columns (Fig. S19†). These observations indicate that transformation of 1*H*-benzotriazole started after favorable conditions (involving *e.g.*, biofilms) had been established in the columns.

3.5 Predictions of TrOC breakthrough in filters with different biochar contents

Dicamba, fipronil, and terbutryn were the only TrOCs that showed breakthrough in the biochar column experiments. The breakthrough data for these TrOCs were fitted to the 1-D contaminant transport model to obtain Freundlich coefficients and exponents (Fig. S20†). Using the transport model with the fit sorption parameters, breakthrough times of the TrOCs in biochar columns were simulated for a bed depth of 0.48 m. The equations and parameters used for modeling the breakthrough curves are shown in eqn S(1)–S(6) and Table S28.† Sorption parameters obtained from fitting the column breakthrough data are shown in Table S29† together with root mean squared errors to evaluate the goodness of fit.

The anionic herbicide dicamba was the most mobile and least retained compound in biochar columns and was therefore chosen as indicator for TrOC breakthrough and filter longevity. Fig. 5a shows simulated dicamba breakthrough curves in biochar columns containing increasing amounts of biochar from one to ten weight percent. Assuming a continuous dicamba influent concentration of 50 $\mu\text{g L}^{-1}$, breakthrough of dicamba (defined as $c/c_0 = 0.2$) was predicted after 1.1×10^3 , 2.6×10^3 , 4.0×10^3 , and 5.3×10^3 pore volumes for columns containing 1, 2.5, 5, and 10 wt% biochar, respectively (Fig. 5a, Table S31†). Greater wt% biochar increases dicamba retention, thus





Fig. 5 (a) Simulated breakthrough curves for dicamba (initial nominal concentration $c_0 = 50 \mu\text{g L}^{-1}$) in 0.48 m columns containing 1 wt%, 2.5 wt%, 5 wt%, and 10 wt% MCG biochar. (b) Simulated breakthrough for dicamba, fipronil, and terbutryn in 0.48 m columns containing 5 wt% MCG biochar (initial nominal concentration $c_0 = 50 \mu\text{g L}^{-1}$).

biochar field applications with >1 wt% are considered beneficial but field tests are needed to assess hydraulic performance and longevity.

In agreement with our column experiments, dicamba breakthrough was followed by fipronil and terbutryn breakthrough with pore volumes of 4.0×10^3 , 1.08×10^4 , and 1.14×10^4 , respectively, for 5 wt% biochar amendment and influent concentrations of $50 \mu\text{g L}^{-1}$ (Fig. 5b). Fipronil removal may be enhanced through transformation processes as indicated by our column experiments (Fig. 4b). Field applications of biochar filters should further screen for the presence of transformation products in the treated stormwater.

Using the dicamba breakthrough predictions shown in Fig. 5a, we assessed the potential lifetime of biochar-amended filters under conditions encountered at a case study site in Los Angeles, CA, USA where $1.1 \times 10^6 \text{ m}^3$ stormwater is planned to be captured and treated over four months during the rainy season. The assumed filter area and depth were 4047 m^2 (1 acre) and 1 m, respectively, resulting in a filter pore volume of approximately $1.6 \times 10^3 \text{ m}^3$ to $2.1 \times 10^3 \text{ m}^3$ for biochar amendments of 1 wt% to 10 wt%, respectively (Table S30[†]). The least retained compound dicamba was used as an indicator substance for early contaminant breakthrough. Influent dicamba concentrations of $50 \mu\text{g L}^{-1}$ were chosen to represent the potential sum of concentrations of mobile trace organic contaminants in urban stormwater runoff. Dicamba breakthrough (defined as $c/c_0 = 0.2$) was predicted to occur after 2, 4, 7, and 10 years for filters amended with 1, 2.5, 5, and 10 wt% of biochar, respectively, at a Darcy velocity of 9 cm h^{-1} (Table S31[†]).

These model simulations suggest a long-term efficiency of biochar filters for the removal of polar and mobile organic contaminants. Lower inflow concentrations of trace organic contaminants in the range of few $\mu\text{g L}^{-1}$ in stormwater runoff will result in longer operation times (5 years and longer) of the biochar filters as demonstrated by model results with dicamba influent concentrations of $5 \mu\text{g L}^{-1}$ (Table S31, Fig.

S21[†]). While our model indicates potential filter operation times of several years or longer, pilot- and full-scale testing under actual field conditions are required to assess treatment performance and longevity, which may be influenced by dynamics in flow rate, stormwater composition, and filter clogging. To sustain the long-term functioning of biochar filters and prevent clogging, stormwater treatment trains should include sedimentation basins and pre-filters for particle removal and regular maintenance of particle removal systems.

4. Conclusions and outlook

The study corroborated that pyrogenic materials like biochar can serve as cost-effective adsorbents for polar organic contaminants in urban stormwater runoff. Among the TrOCs evaluated, dicamba functioned as an early indicator compound for TrOC breakthrough. While anionic organic compounds especially are expected to be poorly retained by biochar, larger sets of organic chemicals need to be investigated to enhance our predictions of contaminant removal from urban stormwater in biochar systems. To date, TrOCs are not part of testing strategies for stormwater treatment materials and devices.⁵³ Unified testing protocols should include a selection of commonly found mobile organic contaminants as well as defined removal targets for improved stormwater treatment performance. Moreover, we need improved criteria for biochar selection. Different gasification biochars or activated biochars should be compared for their capacity for organic contaminant removal from stormwater.

Biochar filters require long-term field testing to improve predictions of treatment efficacy and longevity. Field testing needs to include pretreatment assessments to ensure that the biochar performance is not hampered by particle clogging, as well as performance under conditions of intermittent flow and variable stormwater composition. Mixing of biochar with other low-cost materials may enhance removal of organic and inorganic contaminants including metals and nutrients but field performance has to be evaluated.



Conflicts of interest

There are no conflicts of interest to declare.

Acknowledgements

This research was supported by the National Science Foundation Engineering Research Center for Re-inventing the Nation's Urban Water Infrastructure (NSF ERC ReNUWit 1028968), the UPS Foundation Grant at Stanford University, and the US Department of Defense Strategic Environmental Research and Development Program (ER18-1145). We thank the Stanford Environmental Measurements Facility for training and access to instruments. We further thank the ReNUWit Research Scholar Brian Ly for his help with sampling the column experiments.

Notes and references

- R. P. Schwarzenbach, B. I. Escher, K. Fenner, T. B. Hofstetter, A. C. Johnson, U. von Gunten and B. Wehrli, The challenge of micropollutants in aquatic systems, *Science*, 2006, **313**, 1072–1077.
- J. R. Masoner, D. W. Kolpin, I. M. Cozzarelli, L. B. Barber, D. S. Burden, W. T. Foreman, K. J. Forshay, E. T. Furlong, J. F. Groves, M. L. Hladik, M. E. Hopton, J. B. Jaeschke, S. H. Keefe, D. P. Krabbenhoft, R. Lowrance, K. M. Romanok, D. L. Rus, W. R. Selbig, B. H. Williams and P. M. Bradley, Urban stormwater: An overlooked pathway of extensive mixed contaminants to surface and groundwaters in the United States, *Environ. Sci. Technol.*, 2019, **53**, 10070–10081.
- A. J. Erickson, P. T. Weiss and J. S. Gulliver, *Optimizing Stormwater Treatment Practices*, Springer, New York, 2013.
- G. H. LeFevre, K. H. Paus, P. Natarajan, J. S. Gulliver, P. J. Novak and R. M. Hozalski, Review of dissolved pollutants in urban storm water and their removal and fate in bioretention cells, *J. Environ. Eng.*, 2014, **141**, 04014050.
- F. Linke, O. Olsson, F. Preusser, K. Kümmerer, L. Schnarr, M. Bork and J. Lange, Sources and pathways of biocides and their transformation products in urban storm water infrastructure of a 2 ha urban district, *Hydrol. Earth Syst. Sci.*, 2021, **25**, 4495–4512.
- P. Vega-Garcia, R. Schwerd, C. Scherer, C. Schwitalla, S. Johann, S. H. Rommel and B. Helmreich, Influence of façade orientation on the leaching of biocides from building façades covered with mortars and plasters, *Sci. Total Environ.*, 2020, **734**, 139465.
- M. Huber, A. Welker and B. Helmreich, Critical review of heavy metal pollution of traffic area runoff: Occurrence, influencing factors, and partitioning, *Sci. Total Environ.*, 2016, **541**, 895–919.
- S. Spahr, M. Teixidó, D. L. Sedlak and R. G. Luthy, Hydrophilic trace organic contaminants in urban stormwater: occurrence, toxicological relevance, and the need to enhance green stormwater infrastructure, *Environ. Sci.: Water Res. Technol.*, 2020, **6**, 15–44.
- T. Reemtsma, U. Berger, H. P. H. Arp, H. Gallard, T. P. Knepper, M. Neumann, J. B. Quintana and P. de Voogt, Mind the gap: Persistent and mobile organic compounds – Water contaminants that slip through, *Environ. Sci. Technol.*, 2016, **50**, 10308–10315.
- J. Y. M. Tang, R. Aryal, A. Deletic, W. Gernjak, E. Glenn, D. McCarthy and B. I. Escher, Toxicity characterization of urban stormwater with bioanalytical tools, *Water Res.*, 2013, **47**, 5594–5606.
- Z. Tian, H. Zhao, K. T. Peter, M. Gonzalez, J. Wetzel, C. Wu, X. Hu, J. Prat, E. Mudrock, R. Hettinger, A. E. Cortina, R. G. Biswas, F. V. C. Kock, R. Soong, A. Jenne, B. Du, F. Hou, H. He, R. Lundeen, A. Gilbreath, R. Sutton, N. L. Scholz, J. W. Davis, M. C. Dodd, A. Simpson, J. K. McIntyre and E. P. Kolodziej, A ubiquitous tire rubber-derived chemical induces acute mortality in coho salmon, *Science*, 2021, **371**, 185.
- R. I. L. Eggen, J. Hollender, A. Joss, M. Schärer and C. Stamm, Reducing the discharge of micropollutants in the aquatic environment: The benefits of upgrading wastewater treatment plants, *Environ. Sci. Technol.*, 2014, **48**, 7683–7689.
- J. Margot, C. Kienle, A. Magnet, M. Weil, L. Rossi, L. F. de Alencastro, C. Abegglen, D. Thonney, N. Chèvre, M. Schärer and D. A. Barry, Treatment of micropollutants in municipal wastewater: Ozone or powdered activated carbon?, *Sci. Total Environ.*, 2013, **461–462**, 480–498.
- M. A. Launay, U. Dittmer and H. Steinmetz, Organic micropollutants discharged by combined sewer overflows – Characterisation of pollutant sources and stormwater-related processes, *Water Res.*, 2016, **104**, 82–92.
- L. Mutzner, E. L. M. Vermeirssen, S. Mangold, M. Maurer, A. Scheidegger, H. Singer, K. Booij and C. Ort, Passive samplers to quantify micropollutants in sewer overflows: Accumulation behaviour and field validation for short pollution events, *Water Res.*, 2019, **160**, 350–360.
- A. R. McFarland, L. Larsen, K. Yeshitela, A. N. Engida and N. G. Love, Guide for using green infrastructure in urban environments for stormwater management, *Environ. Sci.: Water Res. Technol.*, 2019, **5**, 643–659.
- D. Tedoldi, G. Chebbo, D. Pierlot, Y. Kovacs and M.-C. Gromaire, Impact of runoff infiltration on contaminant accumulation and transport in the soil/filter media of Sustainable Urban Drainage Systems: A literature review, *Sci. Total Environ.*, 2016, **569–570**, 904–926.
- N. J. Barron, A. Deletic, J. Jung, H. Fowdar, Y. Chen and B. E. Hatt, Dual-mode stormwater-greywater biofilters: The impact of alternating water sources on treatment performance, *Water Res.*, 2019, **159**, 521–537.
- K. Bester and D. Schäfer, Activated soil filters (bio filters) for the elimination of xenobiotics (micropollutants) from storm- and waste waters, *Water Res.*, 2009, **43**, 2639–2646.
- W. Feng, B. E. Hatt, D. T. McCarthy, T. D. Fletcher and A. Deletic, Biofilters for stormwater harvesting: Understanding the treatment performance of key metals that pose a risk for water use, *Environ. Sci. Technol.*, 2012, **46**, 5100–5108.



- 21 S. H. Rommel, V. Ebert, M. Huber, J. E. Drewes and B. Helmreich, Spatial distribution of zinc in the topsoil of four vegetated infiltration swales treating zinc roof runoff, *Sci. Total Environ.*, 2019, **672**, 806–814.
- 22 M. Bork, J. Lange, M. Graf-Rosenfellner, B. Hensen, O. Olsson, T. Hartung, E. Fernández-Pascual and F. Lang, Urban storm water infiltration systems are not reliable sinks for biocides: evidence from column experiments, *Sci. Rep.*, 2021, **11**, 7242.
- 23 K. Zhang, A. Randelovic, D. Page, D. T. McCarthy and A. Deletic, The validation of stormwater biofilters for micropollutant removal using in situ challenge tests, *Ecol. Eng.*, 2014, **67**, 1–10.
- 24 N. Ashoori, M. Teixido, S. Spahr, G. H. LeFevre, D. L. Sedlak and R. G. Luthy, Evaluation of pilot-scale biochar-amended woodchip bioreactors to remove nitrate, metals, and trace organic contaminants from urban stormwater runoff, *Water Res.*, 2019, **154**, 1–11.
- 25 B. A. Ulrich, M. Loehnert and C. P. Higgins, Improved contaminant removal in vegetated stormwater biofilters amended with biochar, *Environ. Sci.: Water Res. Technol.*, 2017, **3**, 726–734.
- 26 S. K. Mohanty, R. Valenca, A. W. Berger, I. K. M. Yu, X. Xiong, T. M. Saunders and D. C. W. Tsang, Plenty of room for carbon on the ground: Potential applications of biochar for stormwater treatment, *Sci. Total Environ.*, 2018, **625**, 1644–1658.
- 27 *Biochar for Environmental Management: Science, Technology and Implementation*, ed. J. Lehmann and S. Joseph, Routledge, London, 2015.
- 28 EBC, European Biochar Certificate – Guidelines for a sustainable production of biochar. Version 9.3E of 11th April 2021, *European Biochar Foundation (EBC)*, Arbaz, Switzerland.
- 29 Y. Tong, P. J. McNamara and B. K. Mayer, Adsorption of organic micropollutants onto biochar: A review of relevant kinetics, mechanisms and equilibrium, *Environ. Sci.: Water Res. Technol.*, 2019, **5**, 821–838.
- 30 S. K. Mohanty, K. B. Cantrell, K. L. Nelson and A. B. Boehm, Efficacy of biochar to remove *Escherichia coli* from stormwater under steady and intermittent flow, *Water Res.*, 2014, **61**, 288–296.
- 31 N. Hagemann, H.-P. Schmidt, R. Kägi, M. Böhler, G. Sigmund, A. Maccagnan, C. S. Mc Ardell and T. D. Bucheli, Wood-based activated biochar to eliminate organic micropollutants from biologically treated wastewater, *Sci. Total Environ.*, 2020, **730**, 138417.
- 32 N. Hagemann, K. Spokas, H.-P. Schmidt, R. Kägi, M. A. Böhler and T. D. Bucheli, Activated carbon, biochar and charcoal: Linkages and synergies across pyrogenic carbon's ABCs, *Water*, 2018, **10**, 182.
- 33 H.-P. Schmidt, A. Anca-Couce, N. Hagemann, C. Werner, D. Gerten, W. Lucht and C. Kammann, Pyrogenic carbon capture and storage, *GCB Bioenergy*, 2019, **11**, 573–591.
- 34 B. A. Ulrich, E. A. Im, D. Werner and C. P. Higgins, Biochar and activated carbon for enhanced trace organic contaminant retention in stormwater infiltration systems, *Environ. Sci. Technol.*, 2015, **49**, 6222–6230.
- 35 M. Uchimiya, L. H. Wartelle, K. T. Klasson, C. A. Fortier and I. M. Lima, Influence of pyrolysis temperature on biochar property and function as a heavy metal sorbent in soil, *J. Agric. Food Chem.*, 2011, **59**, 2501–2510.
- 36 M. Ahmad, A. U. Rajapaksha, J. E. Lim, M. Zhang, N. Bolan, D. Mohan, M. Vithanage, S. S. Lee and Y. S. Ok, Biochar as a sorbent for contaminant management in soil and water: A review, *Chemosphere*, 2014, **99**, 19–33.
- 37 J. E. Grebel, J. A. Charbonnet and D. L. Sedlak, Oxidation of organic contaminants by manganese oxide geomedia for passive urban stormwater treatment systems, *Water Res.*, 2016, **88**, 481–491.
- 38 County of Los Angeles Department of Public Works, Sun Valley Watershed Rory M. Shaw Wetlands park, <https://dpw.lacounty.gov/wmd/svw/docs/Rory-M-Shaw-Wetlands-Park-Fact-Sheet.pdf>, (accessed 9 July 2021).
- 39 D. Werner, U. Ghosh and R. G. Luthy, Modeling polychlorinated biphenyl mass transfer after amendment of contaminated sediment with activated carbon, *Environ. Sci. Technol.*, 2006, **40**, 4211–4218.
- 40 D. Werner, H. K. Karapanagioti and D. A. Sabatini, Assessing the effect of grain-scale sorption rate limitations on the fate of hydrophobic organic groundwater pollutants, *J. Contam. Hydrol.*, 2012, **129–130**, 70–79.
- 41 M. Teixidó, C. Hurtado, J. J. Pignatello, J. L. Beltrán, M. Granados and J. Peccia, Predicting contaminant adsorption in black carbon (biochar)-amended soil for the veterinary antimicrobial sulfamethazine, *Environ. Sci. Technol.*, 2013, **47**, 6197–6205.
- 42 J. P. Kearns, L. S. Wellborn, R. S. Summers and D. R. U. Knappe, 2,4-D adsorption to biochars: Effect of preparation conditions on equilibrium adsorption capacity and comparison with commercial activated carbon literature data, *Water Res.*, 2014, **62**, 20–28.
- 43 G. Zhang, Q. Zhang, K. Sun, X. Liu, W. Zheng and Y. Zhao, Sorption of simazine to corn straw biochars prepared at different pyrolytic temperatures, *Environ. Pollut.*, 2011, **159**, 2594–2601.
- 44 L. Largette, S. Gervelas, T. Tant, P. C. Dumesnil, A. Hightower, R. Yasami, Y. Bercion and P. Lodewyckx, Removal of lead from aqueous solutions by adsorption with surface precipitation, *Adsorption*, 2014, **20**, 689–700.
- 45 M. Teixidó, J. J. Pignatello, J. L. Beltrán, M. Granados and J. Peccia, Speciation of the ionizable antibiotic sulfamethazine on black carbon (biochar), *Environ. Sci. Technol.*, 2011, **45**, 10020–10027.
- 46 A. B. Boehm, C. D. Bell, N. J. M. Fitzgerald, E. Gallo, C. P. Higgins, T. S. Hogue, R. G. Luthy, A. C. Portmann, B. A. Ulrich and J. M. Wolfand, Biochar-augmented biofilters to improve pollutant removal from stormwater – can they improve receiving water quality?, *Environ. Sci.: Water Res. Technol.*, 2020, **6**, 1520–1537.
- 47 H. Genç-Fuhrman, P. S. Mikkelsen and A. Ledin, Simultaneous removal of As, Cd, Cr, Cu, Ni and Zn from stormwater using high-efficiency industrial sorbents: Effect



- of pH, contact time and humic acid, *Sci. Total Environ.*, 2016, **566–567**, 76–85.
- 48 M. Huber, H. Hilbig, S. C. Badenberg, J. Fassnacht, J. E. Drewes and B. Helmreich, Heavy metal removal mechanisms of sorptive filter materials for road runoff treatment and remobilization under de-icing salt applications, *Water Res.*, 2016, **102**, 453–463.
- 49 Z. Reddad, C. Gerente, Y. Andres and P. Le Cloirec, Adsorption of several metal ions onto a low-cost biosorbent: Kinetic and equilibrium studies, *Environ. Sci. Technol.*, 2002, **36**, 2067–2073.
- 50 J.-H. Park, Y. S. Ok, S.-H. Kim, J.-S. Cho, J.-S. Heo, R. D. Delaune and D.-C. Seo, Competitive adsorption of heavy metals onto sesame straw biochar in aqueous solutions, *Chemosphere*, 2016, **142**, 77–83.
- 51 P. He, Q. Yu, H. Zhang, L. Shao and F. Lü, Removal of copper (II) by biochar mediated by dissolved organic matter, *Sci. Rep.*, 2017, **7**, 7091.
- 52 J. P. Chen and S. Wu, Simultaneous adsorption of copper ions and humic acid onto an activated carbon, *J. Colloid Interface Sci.*, 2004, **280**, 334–342.
- 53 C. Dierkes, T. Lucke and B. Helmreich, General technical approvals for decentralised sustainable urban drainage systems (SUDS) – The current situation in Germany, *Sustainability*, 2015, **7**, 3031–3051.

